JOURNAL OF OCULAR PHARMACOLOGY AND THERAPEUTICS
Volume 31, Number 8, 2015

DOI: 10.1089/jop.2015.0049

FEATURED ORIGINAL ARTICLE
2015 Mary Ann Liebert, Inc. publishers Student Travel Award Winner
12th Biennial AOPT Meeting
Charleston, SC

A Simple Optical Coherence Tomography Quantification Method for Choroidal Neovascularization

Rania S. Sulaiman,[1–4] Judith Quigley,[1,2] Xiaoping Qi,[1,2] Michael N. O'Hare,[1,2,5] Maria B. Grant,[1,2] Michael E. Boulton,[1,2] and Timothy W. Corson[1–3,6,7]

Abstract

Purpose: Therapeutic efficacy is routinely assessed by measurement of lesion size using flatmounted choroids and confocal microscopy in the laser-induced choroidal neovascularization (L-CNV) rodent model. We investigated whether optical coherence tomography (OCT) quantification, using an ellipsoid volume measurement, was comparable to standard *ex vivo* evaluation methods for this model and whether this approach could be used to monitor treatment-related lesion changes.

Methods: Bruch's membrane was ruptured by argon laser in the dilated eyes of C57BL/6J mice, followed by intravitreal injections of anti-$VEGF_{164}$ or vehicle, or no injection. *In vivo* OCT images were acquired using Micron III or InVivoVue systems at 7, 10, and/or 14 days post-laser and neovascular lesion volume was calculated as an ellipsoid. Subsequently, lesion volume was compared to that calculated from confocal Z-stack images of agglutinin-stained choroidal flatmounts.

Results: Ellipsoid volume measurement of orthogonal 2-dimensional OCT images obtained from different imaging systems correlated with *ex vivo* lesion volumes for L-CNV (Spearman's $\rho = 0.82$, 0.75, and 0.82 at days 7, 10, and 14, respectively). Ellipsoid volume calculation allowed temporal monitoring and evaluation of CNV lesions in response to antivascular endothelial growth factor treatment.

Conclusions: Ellipsoid volume measurements allow rapid, quantitative use of OCT for the assessment of CNV lesions *in vivo*. This novel method can be used with different OCT imaging systems with sensitivity to distinguish between treatment conditions. It may serve as a useful adjunct to the standard *ex vivo* confocal quantification, to assess therapeutic efficacy in preclinical models of CNV, and in models of other ocular diseases.

Introduction

Choroidal neovascularization (CNV) is the aberrant growth of new blood vessels originating from the choroid into the subretinal space through a break in Bruch's membrane.[1] These new vessels can lead to vascular leakage, hemorrhage, formation of fibrovascular membranes, retinal detachment and eventually, if not treated, to a fibrous scar.

CNV is a major cause of visual loss and is implicated in several neovascular eye diseases such as the wet (or exudative) form of age-related macular degeneration (AMD).[2] Wet AMD is responsible for about 90% of AMD-related blindness in individuals over the age of 55, with about 200,000 new cases diagnosed every year in the United States alone.[3,4] Laser-induced CNV (L-CNV) is a frequently used experimental technique in mice and rats that induces breaks in Bruch's membrane and stimulates blood vessel growth from the choriocapillaris.[5] The resultant CNV resembles aspects of exudative AMD and can easily be performed in rodents, producing robust subretinal vascular lesions within 14 days. L-CNV has become the gold standard in preclinical studies,[6] despite limitations of using rodents.[5] This model has been invaluable for the evaluation of the effects of drug therapies on CNV lesion progression.[7,8]

Vascular endothelial growth factor (VEGF) has been recognized as a key proangiogenic factor in CNV. Targeting

[1]Eugene and Marilyn Glick Eye Institute, Indiana University School of Medicine, Indianapolis, Indiana.
Departments of [2]Ophthalmology, [3]Pharmacology and Toxicology, and [6]Biochemistry and Molecular Biology, Indiana University School of Medicine, Indianapolis, Indiana.
[4]Department of Biochemistry, Faculty of Pharmacy, Cairo University, Cairo, Egypt.
[5]School of Biomedical Science, University of Ulster, Coleraine, Northern Ireland, United Kingdom.
[7]Indiana University Melvin and Bren Simon Cancer Center, Indianapolis, Indiana.

the VEGF pathway, using specific antibodies, antibody fragments, or aptamers, is a standard pharmacotherapeutic approach for wet AMD[9] and has been previously tested in L-CNV experimental models.[10,11] Several methods for 2-dimensional evaluation of L-CNV lesions have been used, including histological analysis and fluorescein angiography.[12] Measuring L-CNV lesion volume using stained choroidal flatmounts *ex vivo* allows the 3-dimensional (3D) measurement of lesion size, which is more informative than measuring lesion area alone and has become widely accepted as a quantitative method to indicate drug efficacy in ameliorating CNV lesions.[5,13,14]

Although *ex vivo* lesion measurements of L-CNV are robust and powerful, *in vivo* imaging analysis of lesions would allow longitudinal studies. Optical coherence tomography (OCT) is a noninvasive, *in vivo* imaging technique that generates high-resolution, cross-sectional images of biological systems.[15] The technique has found extensive use in ophthalmology[15,16] providing detailed images for both the anterior and posterior segments of the eye[17] and has become an essential tool for the clinical evaluation of ocular pathologies, such as wet AMD,[18] retinal tumors,[19–21] and retinal detachment.[22]

Paralleling its rise to clinical prominence, OCT has been used preclinically to monitor disease progression, and OCT images have been shown to be comparable to histological characteristics in disease models,[23–26] including L-CNV.[12,27] However, to our knowledge, 3D quantification of lesions in OCT images has previously used specialized software that is not readily available or compatible with different systems. Moreover, the correlation between calculated lesion volume from OCT images and *ex vivo* choroidal flatmount 3D quantification has not been shown previously. In this study, we show that simple quantification of lesion volumes from OCT images provides reproducible and comparable evaluation to the *ex vivo* analytical methods used in the L-CNV mouse model.

Methods

Animals

All animal experiments followed the guidelines of the Association for Research in Vision and Ophthalmology Statement for the Use of Animals in Ophthalmic and Vision Research and were approved by the Indiana University School of Medicine Institutional Animal Care and Use Committee. Wild-type female C57BL/6J mice, 6–8 weeks of age, were purchased from the Jackson Laboratory (Bar Harbor, ME). These mice were anesthetized by intraperitoneal injections of 17.5 mg/kg ketamine hydrochloride and 2.5 mg/kg xylazine.

Laser-induced model of CNV

Laser photocoagulation was performed as previously described.[28,29] Briefly, eyes were dilated using 1% tropicamide, then underwent laser treatment using 50 μm spot size, 50 ms duration, and 250 mV pulses of an ophthalmic argon green laser, wavelength 532 nm, coupled to a slit lamp. A coverslip was used to allow viewing of the posterior pole of the eye. Each eye received 3 laser burns centered around the optic nerve at 12, 3, and 9 o'clock positions. The laser-induced damage to Bruch's membrane was identified by the appearance of a bubble at the site of laser application. Lesions in which bubbles were not observed were excluded from the study. Where indicated, intravitreal injections of anti-mouse $VEGF_{164}$ neutralizing antibody (R&D Systems, Minneapolis, MN) (5 ng/eye) or vehicle (phosphate-buffered saline) were given immediately after laser in a 0.5 μL volume using a 33-gauge needle. The needle was kept in place for 1 min to prevent the reflux of solution when the needle was removed. Eyes were numbed with tetracaine solution before the injection, and triple antibiotic ointment was used immediately after the injection to prevent infection. A masked researcher undertook imaging and analysis to avoid bias.

Optical coherence tomography

OCT was performed at the indicated times using the Micron III intraocular imaging system (Phoenix Research Labs, Pleasanton, CA) or the InVivoVue OCT system (Bioptigen, Inc., Research Triangle Park, Durham, NC). These are the 2 most commonly used rodent OCT systems. For the Micron system, imaging was done by a single experimenter (R.S.S.). Before the procedure, eyes were dilated with 1% tropicamide solution and lubricated with hypromellose ophthalmic demulcent solution (Gonak) (Akorn, Lake Forest, IL). Mice were then placed on a custom heated stage that moves freely to position the mouse eye for imaging. Several horizontal and vertical images were taken per lesion to allow calculation of CNV lesion volume.

For the InVivoVue system, experiments were done separately by a second laboratory, with imaging conducted by J.Q. Pupils of mouse eyes were dilated with 1% atropine and 2.5% phenylephrine hydrochloride. Mice were then anesthetized. One drop of 2.5% hydroxypropyl methylcellulose was administrated to eyes before examination. Three lateral images (nasal to temporal) were collected, starting at the meridian crossing through the center of the optic nerve head (ONH), and the corresponding L-CNV injury spots were identified by contrasts. Composite fundus images (1.4×1.4 mm, $400 \times 100 \times 1 \times 1$) were taken centered on the ONH. Corresponding high-resolution B-scan (1.4×1.4 mm, $400 \times 400 \times 1 \times 1$) images were then obtained from swept L-CNV spots.

Quantification of lesions as ellipsoids

Quantification was performed as in Fig. 1, for images obtained from the Micron system. The widest sections of the lesions from perpendicular planes were used to calculate ellipsoid volume using the formula $V = \frac{4}{3}\pi abc$ where a, b, and c are the radii of the 3 axes of the ellipsoid. The radii were manually drawn and measured using ImageJ software. The CNV lesion borders were defined from the onset of thickening of the choroidal layer horizontally to the borders of the hyperreflective lesion vertically. The lesion borders were defined similarly for images obtained using the InVivoVue system. In this case, quantitative measures, width (a) and depth (b) of the lesion were measured from the exported central image in B-scanned compositions. The length (c) of the lesions was calculated from en face images as the difference in distance between the beginning and the end of the lesion. Images from both the Micron III and InVivoVue systems were analyzed by 2 independent graders (R.S.S. and M.N.O.) for interobserver comparison.

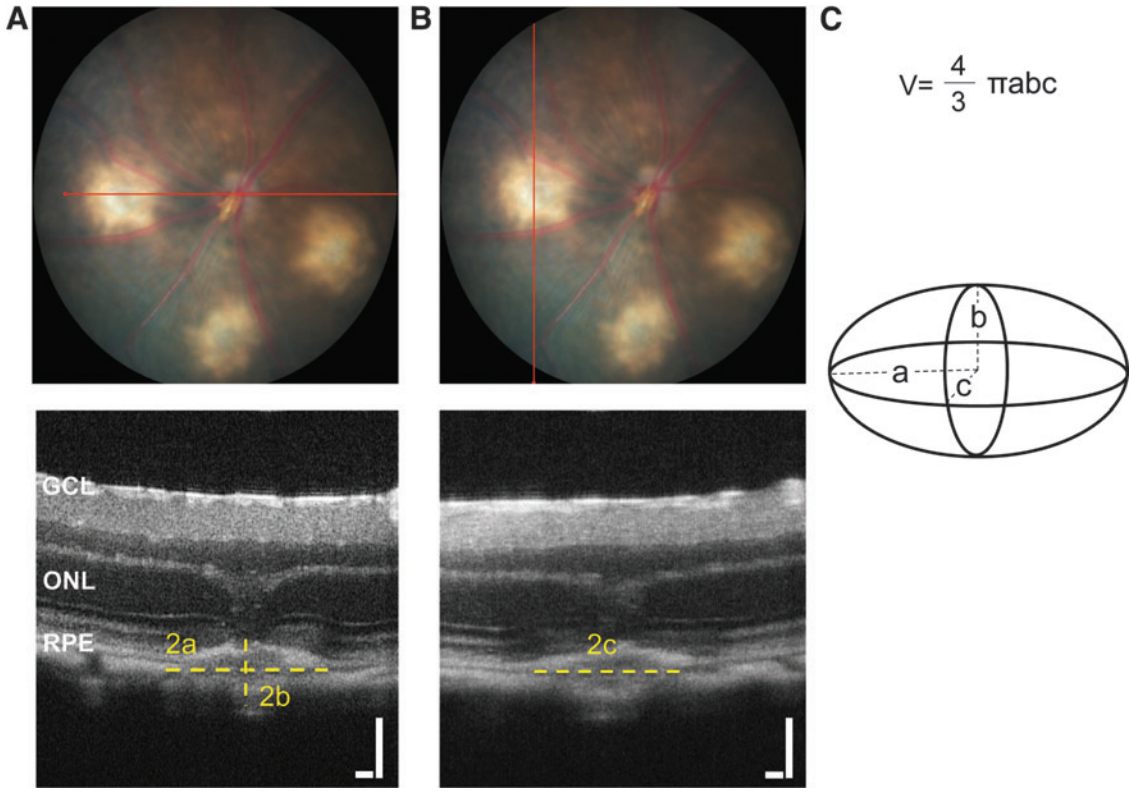

FIG. 1. Determination of ellipsoid axes in Micron OCT images. **(A)** Representative images showing the *horizontal plane* of OCT imaging (*red line*) in the bright-field fundus photographs and the radii *a* (width) and *b* (depth relative to the retina) on the corresponding zoomed-in OCT scan. **(B)** Representative images showing the *vertical plane* in the bright-field image and radius *c* (length) on the corresponding orthogonal zoomed-in OCT scan. **(C)** A schematic diagram showing an ellipsoid with labeled axes corresponding to the OCT images, and the equation used in calculating ellipsoid volume. Scale bars = 100 μm. GCL, ganglion cell layer; OCT, optical coherence tomography; ONL, outer nuclear layer; RPE, retinal pigment epithelium.

The volumes of the 3 lesions in each eye were averaged and considered as an $n = 1$ for statistical analysis.

Choroidal flatmount preparation and ex vivo *CNV lesion volume quantification*

Fourteen days post-laser, L-CNV mice were euthanized by carbon dioxide asphyxiation followed by cervical dislocation. Eyes were enucleated and fixed in 4% paraformaldehyde (PFA) overnight. The anterior segment and the retina were removed, and the remaining retinal pigment epithelium/choroid/sclera was permeabilized by incubation with 0.3% Triton X-100 followed by incubation with rhodamine-labeled *Ricinus communis* agglutinin I (Vector Labs, Burlingame, CA) in the dark for 45 min, to stain blood vessels. The staining step was followed by 2 washes with Tris buffered saline with 0.1% Tween-20 (TBST). Flatmounts of the choroid were prepared and mounted with VECTASHIELD Mounting Medium (Vector Labs) and Z-stack images were taken on an LSM700 confocal microscope (Zeiss, Thornwood, NY). ImageJ software was used to analyze Z-stack images; the summation of the whole stained area in each section, multiplied by the distance between sections (3 μm) was used as an index for the CNV lesion volume.[28] The volumes of the 3 lesions in each eye were averaged and considered as an $n = 1$ for statistical analysis.

Statistical analysis

Statistical analysis was performed with GraphPad Prism 6 software. CNV volume was compared between treatments using the Mann–Whitney test. The Spearman correlation coefficient was used to assess the correlation between lesion volumes measured by OCT and choroidal flatmounts. P values ≤ 0.05 were considered statistically significant.

Results

Ellipsoid quantification in vivo *is comparable to* ex vivo *analysis in L-CNV*

Although Z-stack analysis of wholemounts gives robust and reproducible data, we sought a simple means of evaluating L-CNV lesion volume *in vivo*. Mice underwent OCT 14 days post-laser. Comparing volumetric measurements of OCT and agglutinin-stained wholemount Z-stacks, significant correlation was observed by 2 independent graders; grader 1 with $\rho = 0.79$, $P < 0.01$ and grader 2 $\rho = 0.78$, $P < 0.05$ (Fig. 2). The intraobserver correlation (based on repeated analysis of the same dataset) was $\rho = 0.9$, $P < 0.001$, while the interobserver correlation was $\rho = 0.73$, $P < 0.05$.

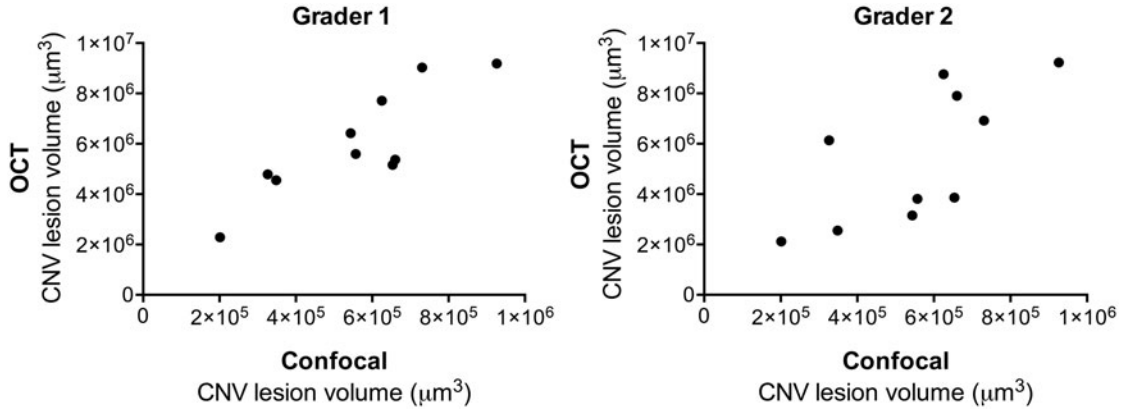

FIG. 2. L-CNV lesion volumes calculated from Micron OCT images obtained 14 days post-laser, analyzed by 2 independent graders, correlate with those calculated based on choroidal flatmount Z-stacks. Grader 1 (*left*) Spearman's $\rho = 0.79$, $P < 0.01$. Grader 2 (*right*) $\rho = 0.78$, $P < 0.05$. $n = 10$. L-CNV, laser-induced choroidal neovascularization.

Ellipsoid quantification is sensitive to different treatment conditions

In the L-CNV model, anti-VEGF antibodies have previously been shown to reduce CNV lesion volume, based on Z-stack image quantification, compared to vehicle-treated controls.[30] We first sought to reproduce this amelioration in the CNV lesion size using the L-CNV mouse model and to compare the difference between treatment groups using both confocal microscopy and OCT. Quantification of CNV lesion volume using the standard Z-stack image method showed the expected significant reduction, about 35%,[31] in lesion volume after anti-VEGF treatment compared to vehicle controls (Fig. 3).

Interestingly, CNV lesion volume calculated using this method from OCT images obtained 7 days after laser and injection also demonstrated a significant reduction, likewise about 35%, after anti-VEGF treatment (Fig. 4). Similar results were obtained from images after 14 days (Fig. 4). Importantly, OCT volume measurements significantly correlated with those measured by Z-stack quantification, after 7 days ($\rho = 0.82$, $P < 0.01$) (Fig. 5A), and after 14 days ($\rho = 0.82$, $P < 0.01$) (Fig. 5B).

Ellipsoid quantification is OCT platform-independent

To validate that our ellipsoidal volume measurement technique could be applied to images from another automated OCT system, we evaluated L-CNV lesions using OCT images obtained with the InVivoVue system. Laser burns were applied to mouse eyes and after 10 days, lesions were evaluated by OCT *in vivo*. Lesion volumes were

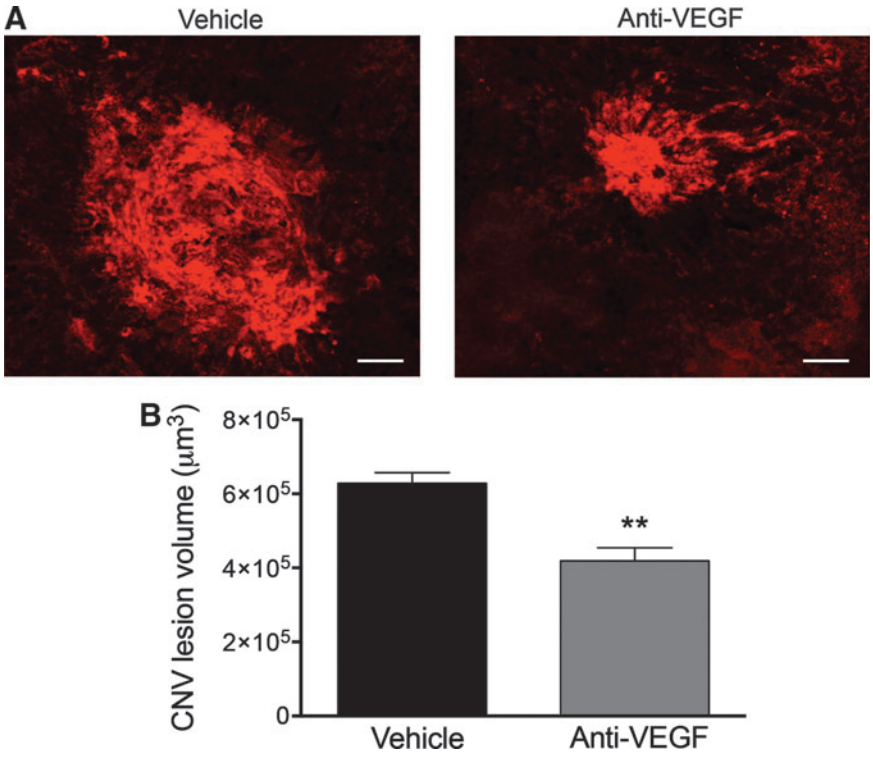

FIG. 3. Choroidal flatmounts stained with agglutinin show a significant reduction in CNV lesion volume after anti-VEGF treatment. **(A)** Representative images from confocal microscopy for CNV lesions from vehicle-treated (*left*) and anti-VEGF-treated eyes (*right*). Scale bars = 50 μm. **(B)** Quantification of the CNV lesion volume from Z-stack images using ImageJ software demonstrated a significant reduction in CNV lesion volume after anti-VEGF intravitreal injection compared to vehicle-treated controls, $^{**}P < 0.01$, Mann–Whitney test. Mean ± SEM, $n = 6$. SEM, standard error of the mean; VEGF, vascular endothelial growth factor.

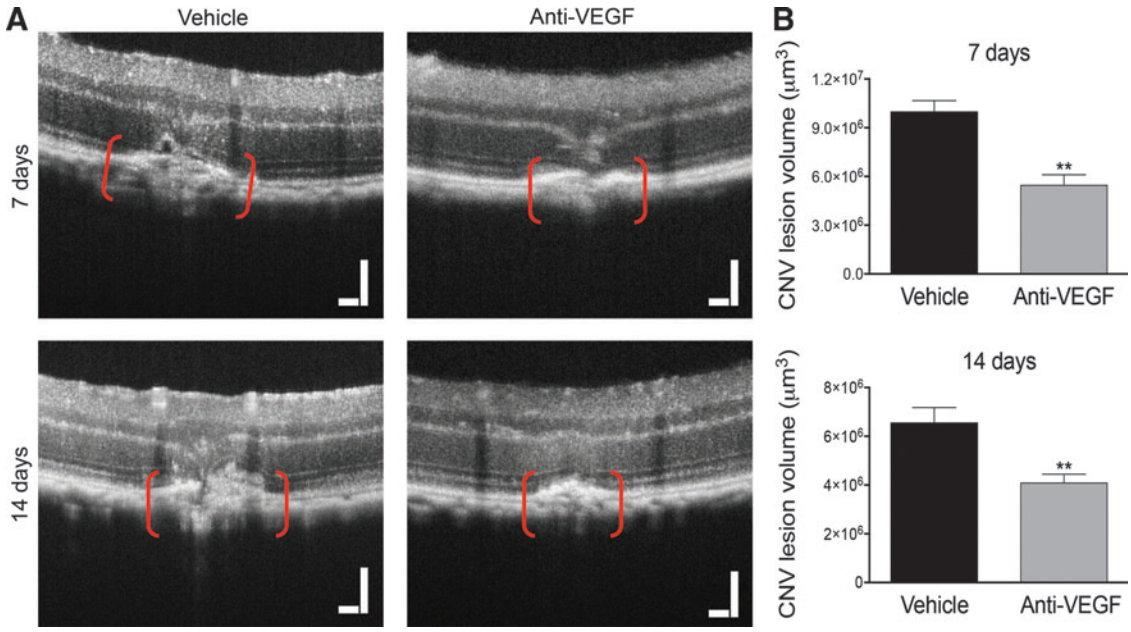

FIG. 4. Quantification of L-CNV lesions by OCT shows a significant reduction in lesion volume after anti-VEGF treatment. **(A)** Representative images of L-CNV lesions, shown between *red brackets*, from vehicle-treated (*left*) and anti-VEGF-treated eyes (*right*) obtained after 7 days (*top*) and 14 days (*bottom*). Scale bars = 100 μm. **(B)** Quantification of the CNV lesion volume calculated as an ellipsoid, showing a significant reduction in CNV lesion volume after anti-VEGF intravitreal injection compared to vehicle-treated controls, after both 7 and 14 days, with $^{**}P < 0.01$, Mann–Whitney test. Note different *y*-axis scales. Mean ± SEM, $n = 6$.

calculated by ellipsoid volume equation, and again compared to volumetric measurements of CNV lesion volumes from agglutinin-stained choroidal flatmounts *ex vivo* after 14 days. Interestingly, a significant correlation was again observed between ellipsoid volume calculation and confocal Z-stack images (Fig. 6) ($\rho = 0.75$, $P < 0.05$). Again, inter-observer variability was modest: data from a second grader yielded similar correlation coefficients. (data not shown). Moreover, removing the peak point, which might be an outlier, did not change the correlation ($\rho = 0.75$, $P < 0.05$).

Discussion

OCT imaging represents an essential adjunct in clinical diagnosis and monitoring of numerous ocular diseases, such as AMD.[32] Evaluation of L-CNV *in vivo* using OCT imaging has been previously studied in different species such as monkeys,[33,34] rabbits,[35] and rats.[27,36,37] Others have evaluated OCT in the mouse model of L-CNV used here by comparing OCT imaging to immunostaining and histological analyses.[12,38,39] However, in this study, we compared for the first time OCT quantification of L-CNV lesions to the robust and commonly used *ex vivo* agglutinin-stained choroidal wholemount quantification method, which allows volumetric measurements of L-CNV lesions through Z-stack sections.[5,13] We saw excellent correlation between the two methods using different OCT imaging systems.

Quantification of OCT images usually requires specialized proprietary software that is not necessarily compatible with multiple imaging systems. In this study, we showed

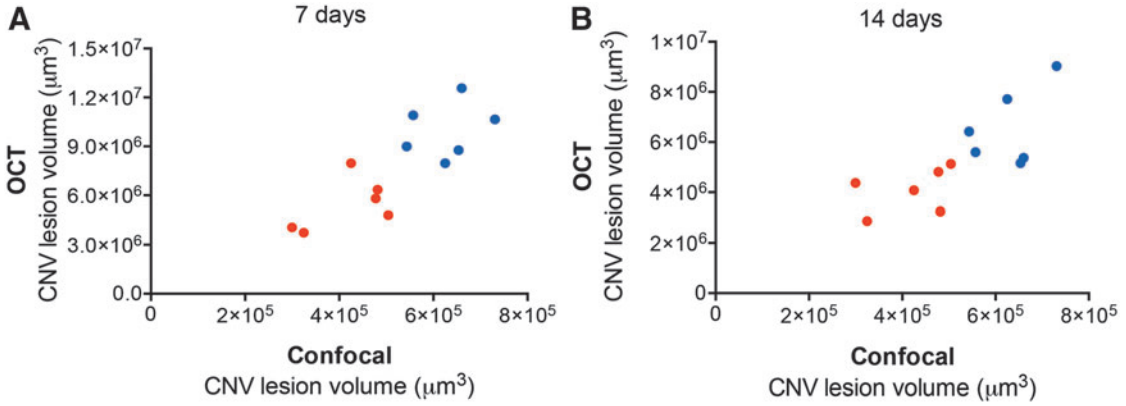

FIG. 5. L-CNV lesion volumes following treatments calculated from Micron OCT images correlate with those calculated based on choroidal flatmount Z-stacks. **(A)** OCT calculations at 7 days, Spearman's $\rho = 0.82$. **(B)** OCT calculations at 14 days, $\rho = 0.82$. Vehicle-treated, *blue*, and anti-VEGF-treated eyes, *red*. $P < 0.01$, $n = 6$ per treatment. Note different *y*-axis scales.

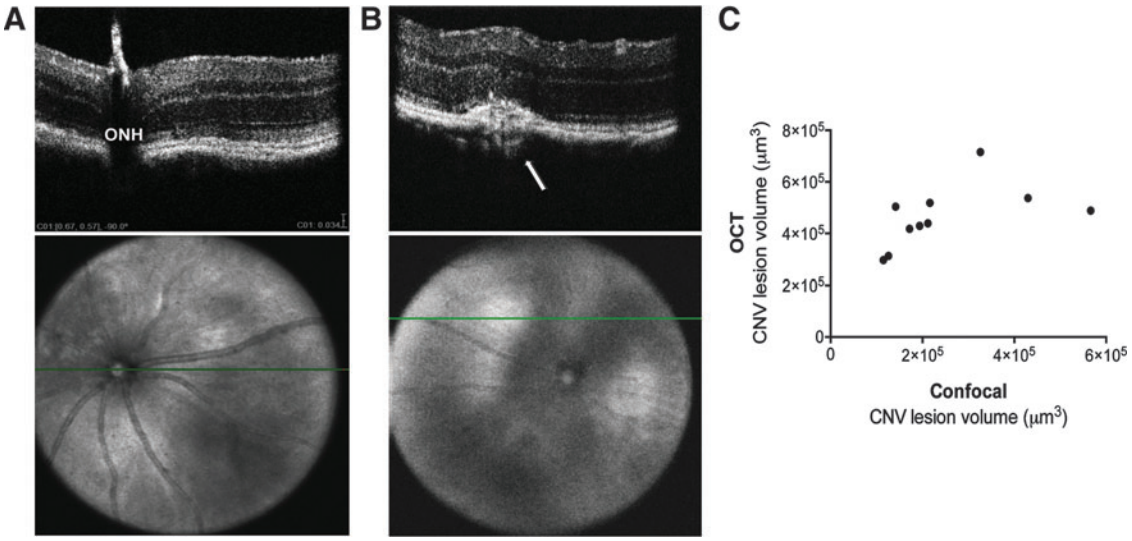

FIG. 6. L-CNV lesion volumes calculated from InVivoVue OCT images obtained 10 days post-laser correlate with those calculated based on choroidal flatmount Z-stacks. **(A)** Representative images showing the horizontal plane of OCT imaging (*green line*) in the en face image and the corresponding B-scan focus on the ONH. Scale bar = 34 μm. **(B)** Representative images showing the en face image and the corresponding B-scan at an L-CNV lesion (*arrow*). **(C)** A significant correlation is observed between 3D measurements of OCT images and confocal Z-stack images, Spearman's $\rho = 0.75$, $P < 0.05$, $n = 10$. ONH, optic nerve head.

that quantitative OCT analysis by a simple method allowed *in vivo* evaluation and monitoring of choroidal lesions in the L-CNV model using two of the most commonly used OCT imaging systems. Although we used ImageJ for analysis, the radii measurements needed for ellipsoid volume could be done using any image-editing program. Quantification of L-CNV lesions, obtained from either Micron or InVivoVue OCT images, using an ellipsoid volume calculation, provides reproducible and comparable results to the standard *ex vivo* quantification method. Consistently, we observed a significant correlation, by two independent graders, between OCT images obtained at days 7, 10, or 14 post-laser, and Z-stack confocal measurements at day 14. However, due to the difference in scaling of the Micron III and InVivoVue imaging systems, calculated lesion volumes by Micron OCT were uniformly larger than those calculated by confocal microscopy. Tissue shrinkage during fixation may also contribute to this finding. Alternatively, since the length of the lesion (dimension *c*) on the InVivoVue was obtained from en face images directly, not from vertical scans as was done with the Micron III system, this might induce some differences in the final calculation. Thus, using the same volumetric measurement system throughout the analysis of an experiment is important.

Our method also applies to OCT imaging to assess pharmacotherapeutic efficacy. In this study, as proof of concept, we used the standard anti-VEGF antibody treatment versus vehicle treatment, to ameliorate CNV lesion volume. To our knowledge, this is the first use of OCT to show therapeutic effect in the murine L-CNV model, although OCT has been used similarly in macaques.[34] As we show, OCT can be used to monitor drug response longitudinally in the same animal, reducing animal usage and enabling time-course comparisons. For instance, we noted that mean L-CNV lesion volumes decreased from days 7 to 14 (Figs. 4 and 5), but the distinction between anti-VEGF and vehicle treatments remained about 35% as previously shown.[31]

OCT analysis is also rapid. Preparation of choroidal flatmounts for the quantification of L-CNV lesion volume is a technically involved and time-consuming technique, requiring at least one overnight step and considerable confocal imaging time, as well as expensive reagents (fluorescent agglutinin in particular).[5] Conversely, acquiring multiple images on an OCT system takes about 5–10 min per eye followed by 5 min for calculation of the lesion volume. Therefore, our ellipsoid volume quantification method represents an inexpensive, rapid, yet reliable quantification method for lesions from OCT images. Despite that, it is important to mention that OCT quantification is not a replacement for the Z-stack confocal measurement. However, it might provide an early prediction of therapeutic effects as well as a second evaluation method for CNV lesion volume.

One limitation of this method is the manual detection of CNV lesion dimensions, which might introduce bias to treatment conditions. However, this can be avoided when the experimenter is masked to treatments throughout imaging and analysis, as well as using at least two independent graders for volumetric analysis. True CNV lesion shape is likely not a simple ellipsoid; therefore, using a simple ellipsoid volume measurement may overestimate irregularly shaped lesions.[39] However, following from this, in experiments comparing CNV lesion-reducing therapies to control conditions, it is likely that our method would be quite conservative (by potentially *overestimating* lesion volume and thus *underestimating* treatment effects), which might be considered as a strength. Like any OCT analysis, our method also requires a clear cornea and lens, and lesions in or near the central retina. This method is also limited to disease models that involve localized lesions that can be demarcated by OCT, such as L-CNV. However, the strength of our method is that it can be used to calculate volumes

from the L-CNV murine model using different automated imaging systems, specifically the Micron and InVivoVue products.

This study provides evidence that OCT is a valuable tool to rapidly and quantitatively evaluate response to drug therapies for CNV using the L-CNV mouse model. Our simple ellipsoidal quantification method may also be applied to the analysis of other focal intraocular lesions and provides rapid analysis for preclinical testing of possible therapeutic agents.

Acknowledgments

This work was supported by the International Retinal Research Foundation, the Retina Research Foundation, and an unrestricted grant from Research to Prevent Blindness, Inc. T.W.C. is supported by NIH KL2TR001106. M.E.B. is supported by R01EY018358. M.B.G. is supported by R01HL110170-03, R01EY007739-23, R01EY012601-15, and R01DK090730-04.

Author Disclosure Statement

T.W.C. has received research and travel support from Phoenix Research Labs. No competing financial interests exist for the other authors.

References

1. de Jong, P.T. Age-related macular degeneration. *N. Engl. J. Med.* 355:1474–1485, 2006.
2. Jager, R.D., Mieler, W.F., and Miller, J.W. Age-related macular degeneration. *N. Engl. J. Med.* 358:2606–2617, 2008.
3. Congdon, N., O'Colmain, B., Klaver, C.C., et al. Causes and prevalence of visual impairment among adults in the United States. *Arch. Ophthalmol.* 122:477–485, 2004.
4. Grossniklaus, H.E., and Green, W.R. Choroidal neovascularization. *Am. J. Ophthalmol.* 137:496–503, 2004.
5. Lambert, V., Lecomte, J., Hansen, S., et al. Laser-induced choroidal neovascularization model to study age-related macular degeneration in mice. *Nat. Protoc.* 8:2197–2211, 2013.
6. Grossniklaus, H.E., Kang, S.J., and Berglin, L. Animal models of choroidal and retinal neovascularization. *Prog. Retin. Eye Res.* 29:500–519, 2010.
7. Dobi, E.T., Puliafito, C.A., and Destro, M. A new model of experimental choroidal neovascularization in the rat. *Arch. Ophthalmol.* 107:264–269, 1989.
8. Sulaiman, R.S., Basavarajappa, H.D., and Corson, T.W. Natural product inhibitors of ocular angiogenesis. *Exp. Eye Res.* 129:161–171, 2014.
9. Prasad, P.S., Schwartz, S.D., and Hubschman, J.P. Age-related macular degeneration: current and novel therapies. *Maturitas.* 66:46–50, 2010.
10. Saishin, Y., Saishin, Y., Takahashi, K., et al. VEGF-TRAP(R1R2) suppresses choroidal neovascularization and VEGF-induced breakdown of the blood-retinal barrier. *J. Cell Physiol.* 195:241–248, 2003.
11. Krzystolik, M.G., Afshari, M.A., Adamis, A.P., et al. Prevention of experimental choroidal neovascularization with intravitreal anti-vascular endothelial growth factor antibody fragment. *Arch. Ophthalmol.* 120:338–346, 2002.
12. Giani, A., Thanos, A., Roh, M.I., et al. *In vivo* evaluation of laser-induced choroidal neovascularization using spectral-domain optical coherence tomography. *Invest. Ophthalmol. Vis. Sci.* 52:3880–3887, 2011.
13. Sengupta, N., Caballero, S., Mames, R.N., et al. The role of adult bone marrow-derived stem cells in choroidal neovascularization. *Invest. Ophthalmol. Vis. Sci.* 44:4908–4913, 2003.
14. Sengupta, N., Caballero, S., Mames, R.N., et al. Preventing stem cell incorporation into choroidal neovascularization by targeting homing and attachment factors. *Invest. Ophthalmol. Vis. Sci.* 46:343–348, 2005.
15. Huang, D., Swanson, E.A., Lin, C.P., et al. Optical coherence tomography. *Science.* 254:1178–1181, 1991.
16. Chen, T.C., Cense, B., Pierce, M.C., et al. Spectral domain optical coherence tomography: ultra-high speed, ultra-high resolution ophthalmic imaging. *Arch. Ophthalmol.* 123: 1715–1720, 2005.
17. Drexler, W., Morgner, U., Ghanta, R.K., et al. Ultrahigh-resolution ophthalmic optical coherence tomography. *Nat. Med.* 7:502–507, 2001.
18. Jia, Y., Bailey, S.T., Wilson, D.J., et al. Quantitative optical coherence tomography angiography of choroidal neovascularization in age-related macular degeneration. *Ophthalmology.* 121:1435–1444, 2014.
19. Espinoza, G., Rosenblatt, B., and Harbour, J.W. Optical coherence tomography in the evaluation of retinal changes associated with suspicious choroidal melanocytic tumors. *Am. J. Ophthalmol.* 137:90–95, 2004.
20. Rootman, D.B., Gonzalez, E., Mallipatna, A., et al. Hand-held high-resolution spectral domain optical coherence tomography in retinoblastoma: clinical and morphologic considerations. *Br. J. Ophthalmol.* 97:59–65, 2013.
21. Shields, C.L., Pellegrini, M., Ferenczy, S.R., and Shields, J.A. Enhanced depth imaging optical coherence tomography of intraocular tumors: from placid to seasick to rock and rolling topography—the 2013 Francesco Orzalesi Lecture. *Retina.* 34:1495–1512, 2014.
22. Wolfensberger, T.J., and Gonvers, M. Optical coherence tomography in the evaluation of incomplete visual acuity recovery after macula-off retinal detachments. *Graefes Arch. Clin. Exp. Ophthalmol.* 240:85–89, 2002.
23. Fischer, M.D., Huber, G., Beck, S.C., et al. Noninvasive, *in vivo* assessment of mouse retinal structure using optical coherence tomography. *PLoS One.* 4:e7507, 2009.
24. Huber, G., Beck, S.C., Grimm, C., et al. Spectral domain optical coherence tomography in mouse models of retinal degeneration. *Invest. Ophthalmol. Vis. Sci.* 50:5888–5895, 2009.
25. Corson, T.W., Samuels, B.C., Wenzel, A.A., et al. Multimodality imaging methods for assessing retinoblastoma orthotopic xenograft growth and development. *PLoS One.* 9:e99036, 2014.
26. Wenzel, A.A., O'Hare, M.N., Shadmand, M., and Corson, T.W. Optical coherence tomography enables imaging of tumor initiation in the TAg-RB mouse model of retinoblastoma. *Mol. Vis.* 21:515–522, 2015.
27. Fukuchi, T., Takahashi, K., Shou, K., and Matsumura, M. Optical coherence tomography (OCT) findings in normal retina and laser-induced choroidal neovascularization in rats. *Graefes Arch. Clin. Exp. Ophthalmol.* 239:41–46, 2001.
28. Qi, X., Cai, J., Ruan, Q., et al. γ-Secretase inhibition of murine choroidal neovascularization is associated with reduction of superoxide and proinflammatory cytokines. *Invest. Ophthalmol. Vis. Sci.* 53:574–585, 2012.
29. Sengupta, N., Afzal, A., Caballero, S., et al. Paracrine modulation of CXCR4 by IGF-1 and VEGF: implications

for choroidal neovascularization. *Invest. Ophthalmol. Vis. Sci.* 51:2697–2704, 2010.
30. Campa, C., Kasman, I., Ye, W., et al. Effects of an anti-VEGF-A monoclonal antibody on laser-induced choroidal neovascularization in mice: optimizing methods to quantify vascular changes. *Invest. Ophthalmol. Vis. Sci.* 49:1178–1183, 2008.
31. Liu, L., Qi, X., Chen, Z., et al. Targeting the IRE1α/XBP1 and ATF6 arms of the unfolded protein response enhances VEGF blockade to prevent retinal and choroidal neovascularization. *Am. J. Pathol.* 182:1412–1424, 2013.
32. Keane, P.A., Patel, P.J., Liakopoulos, S., et al. Evaluation of age-related macular degeneration with optical coherence tomography. *Surv. Ophthalmol.* 57:389–414, 2012.
33. Wang, Q., Lin, X., Xiang, W., et al. Assessment of laser induction of Bruch's membrane disruption in monkey by spectral-domain optical coherence tomography. *Br. J. Ophthalmol.* 99:119–124, 2015.
34. Onami, H., Nagai, N., Machida, S., et al. Reduction of laser-induced choroidal neovascularization by intravitreal vasohibin-1 in monkey eyes. *Retina.* 32:1204–1213, 2012.
35. Koinzer, S., Saeger, M., Hesse, C., et al. Correlation with OCT and histology of photocoagulation lesions in patients and rabbits. *Acta. Ophthalmol.* 91:e603–e611, 2013.
36. Liu, T., Hui, L., Wang, Y.S., et al. *In-vivo* investigation of laser-induced choroidal neovascularization in rat using spectral-domain optical coherence tomography (SD-OCT). *Graefes Arch. Clin. Exp. Ophthalmol.* 251:1293–1301, 2013.
37. Jiao, J., Mo, B., Wei, H., and Jiang, Y.R. Comparative study of laser-induced choroidal neovascularization in rats by paraffin sections, frozen sections and high-resolution optical coherence tomography. *Graefes Arch. Clin. Exp. Ophthalmol.* 251:301–307, 2013.
38. Berger, A., Cavallero, S., Dominguez, E., et al. Spectral-domain optical coherence tomography of the rodent eye: highlighting layers of the outer retina using signal averaging and comparison with histology. *PLoS One.* 9:e96494, 2014.
39. Hoerster, R., Muether, P.S., Vierkotten, S., et al. *In-vivo* and *ex-vivo* characterization of laser-induced choroidal neovascularization variability in mice. *Graefes Arch. Clin. Exp. Ophthalmol.* 250:1579–1586, 2012.

Received: March 31, 2015
Accepted: April 28, 2015

Address correspondence to:
Dr. Timothy W. Corson
Department of Ophthalmology
Indiana University School of Medicine
1160 West Michigan Street
Indianapolis, IN 46202

E-mail: tcorson@iupui.edu